



Molecular dynamics simulation of intragranular Xe bubble re-resolution in UO₂

D. Schwen*, M. Huang, P. Bellon, R.S. Averback

Department of Materials Science and Engineering, University of Illinois at Urbana-Champaign, 1304 W Green St., IL 61801, USA

ARTICLE INFO

Article history:

Received 18 November 2008

Accepted 11 March 2009

ABSTRACT

The homogeneous re-resolution of Xe fission gas bubbles in UO₂ is investigated by combined Monte Carlo and molecular dynamics simulations. Using a binary collision model, based on the Ziegler–Littmark–Biersack potential [J.F. Ziegler, J.P. Biersack, U. Littmark, *The Stopping and Range of Ions in Solids, Stopping and Ranges of Ions in Matter*, vol. 1, Pergamon Press, New York, 1984], the recoil energy distribution of fission gas atoms is obtained. An extensive library of fission gas atom displacement cascades is then compiled using molecular dynamic simulations. It is used for calculating recoil spectrum averaged quantities. The calculations yield a re-resolution parameter for homogeneous re-resolution and a displacement distribution of fission gas atoms around the fission gas bubbles. The results disagree considerably from past estimates. The importance of channeling and threshold energy for fission gas escape are discussed.

© 2009 Elsevier B.V. All rights reserved.

1. Introduction

With the development of generation IV reactor technology, the impact of intragranular fission gas (fg) on the performance of uranium dioxide and mixed oxide fuel elements has gained considerable attention. Gaseous fission products and their precipitation (bubble formation), transport, and segregation are known to adversely influence the thermal and mechanical properties of reactor fuels. Release of gaseous species from the fuel, moreover, can lead to cladding failure at high burn-up. In view of these various deleterious effects of fission gas in fuels, predicting the evolution of the size distribution of fission gas bubbles as a function of temperature and burn-up rate will be crucial in determining fuel performance in advanced future reactors.

The available bubble population models build on two generally accepted fundamental mechanisms for re-resolution of gas atoms from bubbles. One, proposed by Nelson [2] and later termed homogeneous re-resolution, constitutes the interaction of the fission fragments (ff) with fission gas bubbles through energetic collision cascades. Individual fission gas atoms are ejected from bubbles by this mechanism through singular binary collision recoil events. A threshold energy for gas atoms to leave the bubbles is postulated in an *ad hoc* manner. The other, termed heterogeneous re-resolution, and proposed by Turnbull [3], is an unspecified interaction of the fission fragments with entire bubbles, leading to the instantaneous total or partial re-resolution of the contained fission gas in the UO₂ matrix. A comprehensive discussion of analytical bubble population models has been presented by Tucker and White [4] and more recently by Olander and Wongsawaeng [5]. Of interest in this study are models based on the homogeneous re-resolution, such as Ronchi

and Matzke's [6], as well as models that do not explicitly specify the re-resolution mechanism, such as Lösönen's work [7].

The focus of the present work is the homogeneous re-resolution mechanism, and the feasibility of using computer simulations to obtain quantitative data on the re-resolution of Xe atoms. A hybrid approach is employed whereby Monte Carlo (MC) simulations are used to obtain the full recoil energy spectrum of the Xe atoms in intragranular bubbles under fission fragment irradiation, and molecular dynamics (MD) simulations are used to build a library of re-resolution events for these energies. While the MC simulations themselves provide re-resolution information, we choose to verify the data by running full MD simulations within a selected recoil energy window. The lower energy bound coincides with recoils that have a very low re-resolution probability, and are therefore unimportant. The upper energy boundary is set by the practicality of running MD simulations. For recoils above this cut-off, and there are only 2% such recoils, binary collision MC simulation are again employed. As we will show, this introduces negligible error in the calculations.

2. Methodology

2.1. Monte Carlo simulations

For the initial MC part of the study, a new binary collision model (BCM) code was created. It is based on the published TRIM algorithm and uses the Ziegler–Biersack–Littmark (ZBL) universal potential. The software is designed, however, to treat arbitrary sample geometries and arbitrary irradiation conditions, as opposed to the fixed layer geometry and external, monoenergetic, fixed-angle irradiation employed by TRIM (Transport of Ions in Matter) [1]. In either domain of the sample–Xe bubble, or UO₂ matrix–the scat-

* Corresponding author. Tel.: +1 217 244 8678; fax: +1 217 244 2946.
E-mail address: daniel@schwen.de (D. Schwen).

tering events are determined randomly based on the appropriate scattering cross sections. Neither lattice structures nor defect accumulations are taken into account. We used this BCM software [8] to simulate samples of UO_2 containing randomly dispersed spherical bubbles of Xe. Typical Xe bubble sizes and bubble density distributions were employed. The properties of the intragranular bubble population used in the calculations are summarized in Table 1. Although not crucial to this study it should be noted that the bubble population used corresponds to a burnup of 0.01 FIMA or 0.1 Mwd/kgU, with a mean distance between neighboring bubbles of about 14 nm.

The software creates a set of non-overlapping bubbles in a $100 \times 100 \times 100 \text{ nm}^3$ volume with periodic boundary conditions. The identity of the primary knock on atoms (PKA), and the energies of these recoils, were randomly sampled from the known distribution of ^{235}U fission fragments [9]. The locations of the fission events and directions of the fission fragments were chosen randomly. The BCM software follows the cascade event produced by each fission fragment until all atoms have fallen below a given threshold energy, 100 eV in the present case. At each simulation step a collision test is performed against the bubble set. Every energy transfer to a Xe atom is recorded, thus generating a recoil energy histogram for Xe atoms; an example is shown in Fig. 1. All Xe recoils that receive an energy of more than 200 eV and less than 12 keV are tagged. The recoil energy histogram of the subset of tagged atoms (solid black curve in Fig. 1) is used as input data for the MD simulations. All Xe atoms in subcascades of flagged atoms are kept unflagged (dashed black curve in Fig. 1); they correspond almost exclusively to secondary Xe recoils inside bubbles. The gray curve in Fig. 1

sums all Xe recoils outside the aforementioned energy window. The high energy side of this distribution contains about 2% of all Xe recoils, while the low energy end contains less than 50% of all Xe recoils. All Xe displacements, relative to their respective bubbles of origin, are stored, generating a displacement distance histogram purely from MC data. Furthermore, the energy deposition due to phonon excitations is spatially mapped around the Xe bubbles. This is done for later analysis of possible effects of thermal spikes.

2.2. Molecular dynamics

The LAMMPS code [10] was employed for the molecular dynamics using the Particle-Particle Particle-Mesh (PPPM) method for treating the long-ranged coulomb interactions between the oxygen and uranium atoms. The non-coulombic pair interactions and their first derivative were tabulated with a smooth cut-off up to 1.04 nm. Periodic boundary conditions were used for all simulation runs. The choice of a potential for the MD simulations is constrained by the size and ensuing computational cost of the simulation volumes. The setups in this work dictated the choice of a simple rigid-ion potential over a more complex core-shell potential. For the U-U, U-O, and O-O interactions, we used the potential by Morelon et al. [11] based on a recent review of UO_2 potentials by Govers et al. [12]. The Morelon potential was developed primarily for the simulation of displacement cascades in UO_2 lattices and builds on work by Sindzingre [13] and Karakasidis [14]. The charges on the uranium and oxygen atoms are taken to be fixed, but fractional (i.e. non-integer). In addition to the coulomb contribution, the U-O interaction contains a Born-Meyer-Huggins covalent bonding contribution and the O-O interaction contains a piece-wise patched function connecting a Born-Mayer part, two polynomials and $1/r_{ij}^{-6}$ long-range tail (r_{ij} being the interatomic distance). The U-U interaction is assumed to be dominated by the strong electrostatic repulsion and is therefore taken to be purely coulombic. The fixed ionic charges are expected to enhance the recrystallization to the fluorite structure, the drive for local charge neutrality entails the local preservation of the UO_2 stoichiometry.

The Morelon potential reproduces the lattice parameter across a broad temperature range. It underestimates the heat capacity by about a factor of two, however, among comparable potentials it comes closest to the experimental data. The potential reproduces the melting of the oxygen sublattice (Bredig transition [15]) at 2000 K. The isothermal bulk modulus of UO_2 is well reproduced for temperatures above 1600 K. All of our simulations were carried out at a matrix temperature of 1600 K, which is a typical fuel element centerline temperature under normal operating conditions. Govers et al. report an over prediction of the melting temperature of UO_2 by 300–400 K. Our own tests, however, put the melting point at about 3300 K, which is only ≈ 150 K above the accepted value of the melting point, 3150 K.

The Xe-U potential is of the Born-Meyer form, the Xe-Xe and Xe-O interactions are modeled using Lennard-Jones potentials, the parameterization for all three interactions is taken from a recent work by Geng et al. [16]. All interactions are splined to the universal ZBL potential for short ranges. High energy scattering kinematics is determined by the ZBL parts of the interaction potential.

The low energy portions of the potential reproduce the structure, including sub-lattice and total melting points and determine the late portions of the displacement cascades. Channeling is expected to occur in the characteristic open fluoride, affecting the scattering and ranges of fission gas atoms.

Several Xe recoil energies within the 200 eV–12 keV window were chosen for simulation (200 eV, 400 eV, 1000 eV, 1500 eV,

Table 1
Properties of the intragranular bubble population used in the calculations.

Symbol	Definition	Value
N_b	Bubble density	$7.4 \times 10^{-4} \text{ nm}^{-3}$
r_b	Bubble radius	1 nm
ρ_{Xe}	Xe density in bubbles	20 atoms/ nm^3 (4.2 g/ cm^3)
F	Fission-rate density	$10^{-8} \text{ nm}^{-3} \text{ s}^{-1}$

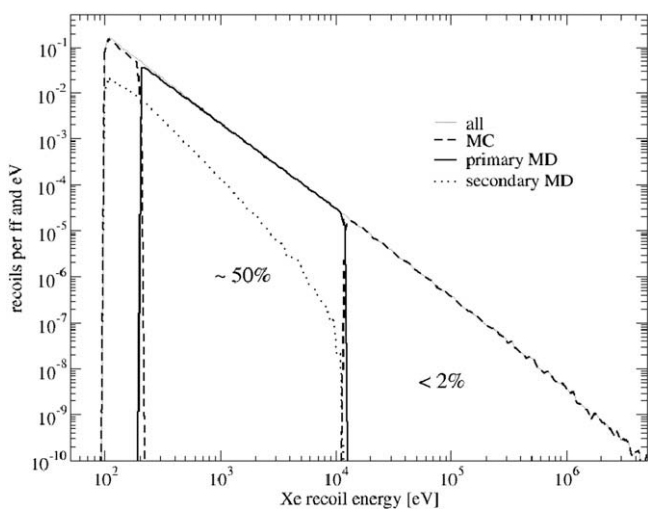


Fig. 1. Spectrum of Xe recoil energies obtained from the MC simulation. The solid black curve sums up all events in which the Xe atom receives an energy greater than 200 eV but less than 12 keV from either the fission fragment or O and U recoils, or from a Xe recoil with an energy larger than 12 keV. These are the events that are treated by the MD simulation. The dotted black curve are secondary Xe recoils inside a bubble. The dashed black curve sums up all Xe recoils outside the aforementioned energy window. The high energy side contains about 2% of all Xe recoils, while the low energy end contains less than 50% of all Xe recoils.

2 keV, 4 keV, and 10 keV) and for each a cubic volume containing a UO_2 lattice was created. The overall size of the simulation box was chosen such that the recoil energy does not exceed 1/20 eV per atom, thus preventing unrealistic heating of the cell. A spherical void was created in the UO_2 lattice by stoichiometrically removing atoms, and thereby preserving the overall charge neutrality of the system. The void was filled with a close-packed Xe lattice, and the system was relaxed at 1600 K for 70–125 ps. After relaxation the Xe gas density in the bubble was determined to be about 3.4 g/cm³ with bubble diameter of 2 nm, which is in good agreement with reported experimental densities [17]. The bubbles remain compact and spheroidal, no Xe atoms were observed leaving the bubble during annealing. No long-range order was observed in the Xe.

For each cascade, a Xe atom inside the bubble was randomly selected and assigned the predetermined kinetic energy, sample from the distribution in Fig. 1, with a random direction. Out of the entire displacement cascade produced by the fission fragment only the subcascades created by the Xe recoils inside fission gas bubbles are simulated. The omission of high energy displacements produced in the UO_2 lattice by the fission fragment allows both the choice of longer simulation time steps due to a lower maximum velocity in the simulation volume as well as the use of a smaller simulation volume, reducing the computational cost per simulated displacement cascade initiated by Xe recoils. This omission of lattice recoils has negligible effect on the outcome.

Our simulation scheme neglects any possible displacement events that bring lattice material into the gas bubbles. Uranium and oxygen atoms knocked into the Xe bubbles are expected to quickly move to the bubble walls due to coulomb attraction by the inhomogeneously distributed charge. The rates of such atom knock-in's are comparable to the rates of atoms being knocked-out, which helps to keep the intra-bubble pressure in balance. Knock-ins of re-solved Xe atoms are not considered due to their negligible probability. Our approach also neglects overlapping displacement events either from two successive fission fragments or from subcascades of a single fission fragment. The time between successive fission fragment cascades in real fuel in operation is sufficiently long to restore local thermal equilibrium, while the time difference between nearby events in the same displacement cascade is short enough so that the lattice is not much disturbed during flight of the recoiling Xe atom. The Xe atoms thus recoil into a virtually undisturbed surrounding lattice.

3. Results

A set of 400 recoil events per energy was simulated, and the final distribution of all Xe atom distances around the bubble center recorded. Wrap around due to the periodic boundary conditions and the finite simulation volume was encountered in roughly 10% of all simulation runs; it was accounted for by unfolding the full trajectory data for the xenon atoms. No events where the knocked-out atom crosses the simulation volume boundary and re-enters the bubble were observed. Fig. 2 shows for various energies the histogram of Xe atom re-solution distances, measured from the centers of their bubbles of origin. The probability of resolving a Xe atom decays faster than exponentially with distance. The high Xe intensities at short distances from the bubble center correspond to the onset of the Xe bubble surface.

The conditions for the loss of a Xe atom from the bubble can be characterized by a threshold energy. For example, Fig. 3 shows the probability for Xe atoms leaving the 'radius of influence' of its nascent bubble, as a function of Xe recoil energy. Three curves for radii of influence of 1.5, 2.0, and 2.5 nm are plotted, the bubble radius being 1 nm. The threshold behavior is recognized by the rapid

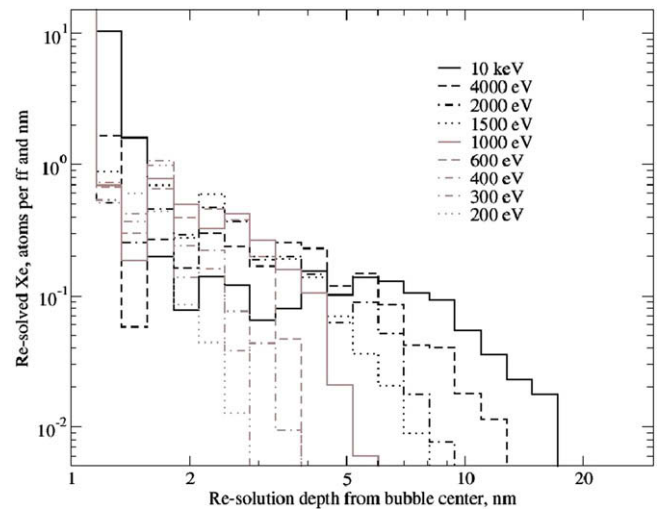


Fig. 2. Histogram of displacement lengths of Xe atoms from the centers of their bubbles of origin, compiled from a library of MD simulations for various Xe recoil energies.

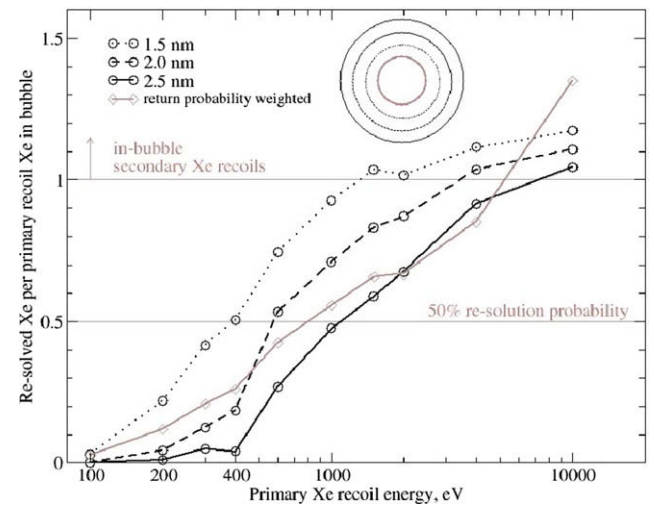


Fig. 3. Probability for Xe atoms to leave a 'radius of influence' of their bubble of origin, as a function of Xe recoil energy. Bubble radius is 1 nm, curves for radii of influence of 1.5, 2.0 and 2.5 nm are plotted. The data in the gray curve with diamond symbols is corrected for back-diffusion using a simple return probability (r_b/r) model. Re-solution in excess of unity is achieved by intra-bubble recoils leading to the knock-out of more than one Xe atom.

increase in the probability of a Xe atom being re-solved as the primary recoil energy increases above 300–400 eV. This observation is, in fact, in good agreement with the *ad hoc* threshold energy of 300 eV postulated in the homogeneous re-solution model by Nelson [18]. The radius of influence can be estimated by back-diffusion probability. Disregarding the possible strain fields of the bubbles, the independent sink approximation [19] can be utilized, taking the bubbles as sinks with radius r_b (bubble radius) for the Xe atoms. The probability for a Xe atom to be recaptured by its bubble of origin is given simply by r_b/r , the timescale for the recapture to occur depends on the effective diffusion constant but this is not considered in the present work. Below a distance of $2 \times r_b$ from the center of the bubble of origin, the recapture probability is greater than 50%, and beyond this distance, it asymptotically goes to zero. This suggests assuming the 'radius of influence' to be twice the bubble radius, and considering only atoms removed beyond this distance as 'removed'. For recoils below 200 eV, virtually no

Xe atom leaves a bubble. At recoil energies above 4 keV the number of re-solved atoms per recoil becomes larger than unity, signifying the onset of secondary Xe recoils leaving the bubble.

The final step in the dual MC/MD approach is the summation of the Xe atom displacement histograms derived from MD, weighted by the probability densities of the recoil energies, as obtained from MC.

Fig. 4 shows a comparison of the weighted summation from MD/MC (solid black line) and the displacement histogram from the MC simulation alone (dashed black line). At small displacement distances, the two curves are quite similar; it is only at larger distances that they show significant differences. We attribute this difference to channeling, as we discuss in detail below. Recoil energies outside of the 200 eV–12 keV window were not simulated by MD. The gray dashed curve contains the MC long-range contribution from the recoils with energies greater than 12 keV, the gray dotted curve contains the MC contribution arising from the recoils with energies below 200 eV; it does not take the threshold energy for atom removal from the bubbles into account.

The possibility of channeling was investigated by generating ‘trajectory element’ histograms in direction space. The trajectories of all Xe atoms that were removed from bubbles were cut into short linear segments, corresponding to the atom movement over 100 simulation steps. The orientation of these segments with respect to the surrounding UO_2 lattice and their lengths were calculated. The top graph in Fig. 5 shows a probability histogram of Xe path element lengths occurring in a certain direction, compiled from all 10 keV cascade events. Three peaks along the $[1\ 1\ 0]$ directions are visible, indicating preferential movement along the $[1\ 1\ 0]$ direction. This direction is the dominant channeling direction in face centered cubic (fcc) lattices, and thus consistent with the U sub-lattice having a fcc structure. It can be assumed that the light O ions do not significantly contribute to channeling.

The peaks in Fig. 5 become clearer when instead of path element lengths the change in distance to the bubble center is plotted (bottom graph). The probability histogram now indicates which directions of movement contribute most to removal of Xe atoms from the bubbles. Diffusive jumps of Xe after re-resolution from the bubbles as well as thermal vibrations do not sum up to

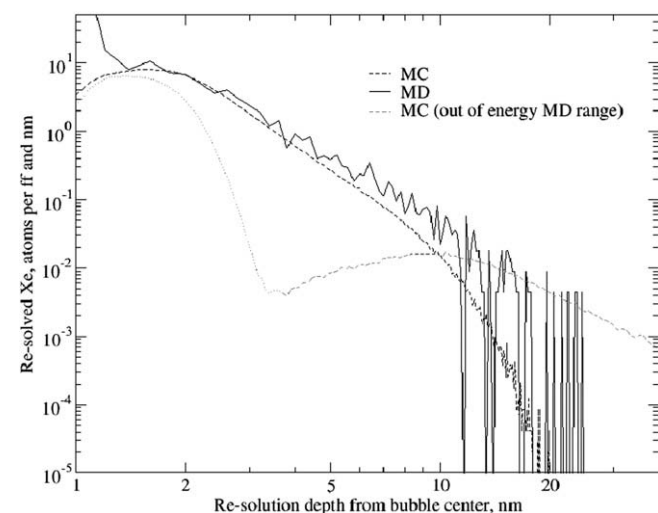


Fig. 4. Xe atom displacement histograms obtained from both the MC simulation (dashed black line) and from the MD simulation as a weighted average of the cascade runs for all Xe recoils in the energy range above 200 eV and below 12 keV (solid black line). The difference between the MC and MD ranges may be attributed to channeling in the open fluoride structure. The gray dashed curve contains the MC long-range contribution from the >12 keV recoils, the gray dotted curve contains the MC contribution from the <200 eV recoils, which does not take the threshold energy for atom removal from the bubbles into account.

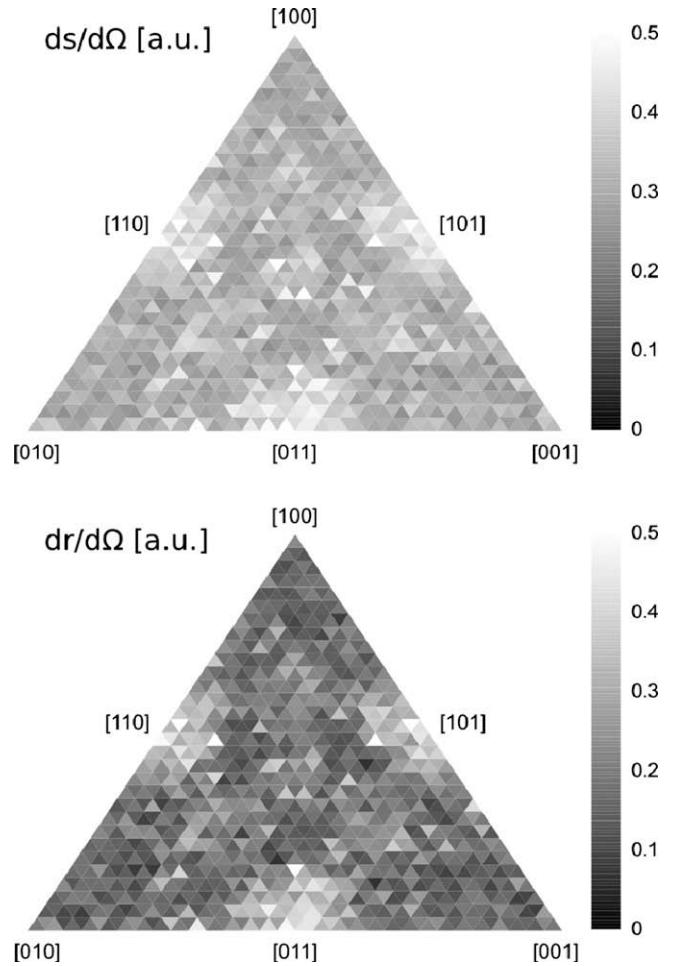


Fig. 5. Top graph shows a histogram of Xe path element lengths ds in direction space, with $d\Omega$ being the spatial angle element. Each path element corresponds to the movement of a Xe atom over a few femtoseconds. Three peaks along the $[1\ 1\ 0]$ directions are visible. The peaks become clearer when instead of path element length the change in distance dr to the bubble center is plotted (bottom graph). Diffusive movement which does not contribute to a change in total displacement length shows not up in this dataset.

a change in total displacement length when averaged over a large set of Xe recoils. This removes a background from the dataset and isolates the channeling contribution.

4. Discussion and conclusions

The dual MC/MD approach yields insight into the homogeneous bubble re-resolution mechanism that can not be readily obtained by experiment. For example, previously *ad hoc* postulated parameters could be tested within the limits of the interatomic potential and the approximations made in this study. In our model system (summed up in Table 1), consisting of 1 nm radius bubbles and bubble number density of $7 \times 10^{-4} \text{ nm}^{-3}$, five Xe atoms are removed from bubbles per fission fragment. Given a typical fission rate density of $10^{-8} \text{ nm}^{-3} \text{ s}^{-1}$ this results in 4×10^{-5} fission gas atom knock-outs per bubble s^{-1} . Each bubble contains about 80 atoms, yielding a re-resolution parameter b_{hom} of about $3 \times 10^{-6} \text{ s}^{-1}$ fission gas knock-outs per fission gas atom, a number that is a factor of ≈ 50 lower than Nelson’s revised analytical results [2]. This discrepancy is rooted in the Xe recoil energy spectra used for the fission gas re-resolution calculations (Fig. 1). Nelson’s primary recoil spectrum shows higher intensities up to a factor of two above the results from our calculations for energies below

10 keV. For the secondary recoil spectrum, Nelson's intensity estimate is greater by a factor of ≈ 40 than our results. We expect that our Monte Carlo BCM calculations, which are based on the experimentally verified ZBL potential, are far more accurate than the previously used analytical approach using coulomb potentials in the hard-sphere approximation. Moreover, the spectrum averaged recoil distribution for a fission fragment or recoil atom slowing down in the UO_2 is obtained naturally in the MC simulation considering both nuclear as well as electronic stopping, but it can be an additional source of error in analytical calculations. The approach of building a cascade library using MD simulation also takes care of ion channeling, and provides good accuracy in the low energy region, where continuum binary collision models break down. Furthermore our calculation also takes into account intra-bubble stopping of fission fragments; the resulting re-resolution parameter dependence on the bubble size, however, will be discussed elsewhere. Lösönen [7] obtains a re-resolution parameter of about $5 \times 10^{-4} \text{ s}^{-1}$ fission gas knock-outs per fission gas atom by fitting his model to experimental bubble size distribution data by Baker [20]. While Lösönen does not explicitly assume either a homogeneous or heterogeneous re-resolution mechanism in his model, and his method of obtaining the re-resolution parameter is indirect, it still seems that his re-resolution cannot be explained by single fg atom knock-outs.

It should be stressed that the assignment of a 'radius of influence' to determine escape from the bubble is an artificial measure to obtain a value for the re-resolution parameter for comparison with previous results. Our data set includes a Xe intensity dependence on the re-resolution distance, and may thus be useful as a re-resolution

source-term in a further study of fission gas population development using methods such as kinetic Monte Carlo simulation or phase field modeling which do not use the concept of a 'radius of influence'.

Acknowledgments

The research was supported by the US Department of Energy, under NERI-C Award No. DE-FG07-14891.

References

- [1] J.F. Ziegler, J.P. Biersack, U. Littmark, *The Stopping and Range of Ions in Solids, Stopping and Ranges of Ions in Matter*, vol. 1, Pergamon Press, New York, 1984.
- [2] R.S. Nelson, *J. Nucl. Mater.* 31 (1969) 153.
- [3] J. Turnbull, *J. Nucl. Mater.* 38 (1971) 203.
- [4] R.J. White, M.O. Tucker, *J. Nucl. Mater.* 118 (1983) 1.
- [5] D.R. Olander, D. Wongsawaeng, *J. Nucl. Mater.* 354 (2006) 94.
- [6] C. Ronchi, H.J. Matzke, *J. Nucl. Mater.* 45 (1972/73) 15.
- [7] P. Lösönen, *J. Nucl. Mater.* 304 (2002) 29.
- [8] The Source Code of the New TRIM Implementation. Available from: <http://groups.mrl.uiuc.edu/averback/3dtrim>.
- [9] H.R. Faust, *Eur. Phys. J. A* 14 (2002) 459.
- [10] S.J. Plimpton, *J. Comp. Phys.* 117 (1995) 1.
- [11] N.-D. Morelon, D. Ghaleb, J.-M. Delaye, L.V. Brutzel, *Phil. Mag.* 83 (2003) 1533.
- [12] K. Govers, S. Lemehov, M. Hou, M. Verwerft, *J. Nucl. Mater.* 376 (2008) 66.
- [13] P. Sindzingre, M.J. Gillan, *J. Phys. C: Solid State Phys.* 21 (1988) 4017.
- [14] T. Karakaidis, P.J.D. Lindan, *J. Phys.: Condens. Matter* 6 (1994) 2965.
- [15] A.S. Dworkin, M.A. Bredig, *J. Phys. Chem.* 72 (1968) 1277.
- [16] H.Y. Geng, Y. Chen, Y. Kaneta, M. Kinoshita, *J. Alloys Compd.* 457 (2008) 465.
- [17] K. Nogita, K. Une, *J. Nucl. Mater.* 250 (1997) 244.
- [18] R.S. Nelson, *J. Nucl. Mater.* 25 (1968) 227.
- [19] K. Schröder, *Springer Tract Modern Phys.* 87 (1980) 218.
- [20] C. Baker, *J. Nucl. Mater.* 66 (1977) 283.